



# Activity standardization of $^{99m}\text{Tc}$ using liquid scintillation counting method

K. B. Lee<sup>1</sup> · Jong Man Lee<sup>1</sup> · Tae Soon Park<sup>1</sup> · Sang Han Lee<sup>1</sup>

Received: 9 October 2017 / Published online: 27 April 2018  
© Akadémiai Kiadó, Budapest, Hungary 2018

## Abstract

The Korea Research Institute of Standards and Science (KRISS) participated in the BIPM.RI(II)-K4.Tc-99 m comparison of activity measurements of  $^{99m}\text{Tc}$ . We develop the national primary standard for  $^{99m}\text{Tc}$  solution used during the comparison. We use two primary liquid scintillation counting techniques for the standardization: digital coincidence counting with the  $4\pi\beta(\text{LS})-\gamma(\text{NaI}(\text{Tl}))$  system and triple-to-double coincidence ratio counting. Both methods give consistent results for the specific activity of a  $^{99m}\text{Tc}$  solution. Adopting the result from the DCC method as the reference value of the  $^{99m}\text{Tc}$  measurement, we evaluate the standard uncertainty of 0.856% for the KRISS primary standard of the  $^{99m}\text{Tc}$  activity. The K4 comparison result shows that the newly-established KRISS primary standard lies within the standard uncertainty with the key comparison reference value defined from other  $^{99m}\text{Tc}$  measurements.

**Keywords** Digital coincidence counting · Triple-to-double coincidence ratio · Technetium-99m · Liquid scintillation counting

## Introduction

The metrological comparability of  $^{99m}\text{Tc}$  measurements is hard to establish because of the low energy of its emitted radiation in coincidence with gamma rays as well as its short half-life. The short half-life of  $^{99m}\text{Tc}$  prevented the Korea Research Institute of Standards and Science (KRISS) from sending a  $^{99m}\text{Tc}$  ampule for measurement in the International Reference System (SIR) at the Bureau International des Poids et Mesures (BIPM). A transfer instrument of SIR (SIRTI) has been developed at BIPM, allowing KRISS to establish the comparability in Korea for  $^{99m}\text{Tc}$  measurements. Second to the National Institute of Standards and Technology, KRISS participated in the BIPM.RI(II)-K4.Tc-99m comparison of activity measurements of  $^{99m}\text{Tc}$  that was held at the KRISS in September 2010. This paper describes the national primary standard for  $^{99m}\text{Tc}$  activity calibrating the reference ionization

chamber that actually measured the  $^{99m}\text{Tc}$  solution used during the comparison.

We measure the activity of a  $^{99m}\text{Tc}$  solution using two liquid scintillation (LS) counting methods: digital coincidence counting (DCC) with the  $4\pi\beta(\text{LS})-\gamma(\text{NaI}(\text{Tl}))$  system [1, 2] and triple-to-double coincidence ratio (TDCR) counting [3]. Two kinds of LS cocktails are used to investigate the dependence of our measured activity on the LS solvent used: pseudocumene-based Hionic Fluor and DIN-based Ultima Gold. The  $4\pi\beta(\text{LS})-\gamma(\text{NaI}(\text{Tl}))$  system operated in DCC mode acquires the pulse-height spectra for the LS and NaI channels for each LS source prepared. This method gives a reported activity value with the relative standard uncertainty of 0.856%, the dominant component of which is due to the reproducibility with the fit ranges used. The compatibility of the measured activity is established by comparisons of the result with those obtained with the TDCR method and the ionization chamber method. In the TDCR method the double-coincidence efficiency and triple-coincidence efficiency are calculated on the basis of the Poisson distribution for the number of photoelectrons in the photomultiplier (PM) tubes. The K4 comparison result shows that the KRISS primary standard for  $^{99m}\text{Tc}$  activity lies within the standard

✉ K. B. Lee  
lee@kriss.re.kr

<sup>1</sup> Korea Research Institute of Standards and Science,  
Daejeon 34113, Republic of Korea

uncertainty with the key comparison reference value, defined from other  $^{99m}\text{Tc}$  measurements.

## Experimental

### Source preparation

The master solution used for the measurements has a nominal  $^{99m}\text{Tc}$  activity of 100 MBq in 5 mL of NaCl solution. We use two kinds of LS cocktails of DIN-based Ultima Gold and pseudocumene-based Hionic Fluor allowing investigation of the dependence of our measured activity on the LS solvent used. A total of ten LS sources, i.e., five sources for each cocktail, are prepared: four active sources and one blank source. Aliquots of  $^{99m}\text{Tc}$  solution are dispensed, after gravimetric determination, into eight 22 mL borosilicate glass vials previously filled with 10 mL of LS cocktail. For background measurements the two blank sources are also prepared by adding the scintillant only in the vials.

### Digital coincidence counting with the $4\pi\beta(\text{LS})-\gamma(\text{NaI}(\text{Tl}))$ system

We measure the activity of the  $^{99m}\text{Tc}$  sources prepared using the  $4\pi\beta(\text{LS})-\gamma(\text{NaI}(\text{Tl}))$  system. Considering the short half-life of  $^{99m}\text{Tc}$ , we take the digital data from the system to reduce the counting time by acquisition system allows us to perform multiple analyses of a given counting data set with different analysis parameter. The  $\beta-\gamma$  coincidence counts are recorded using the arrival time differences between the two sequences of detector pulses: the pulses from the liquid scintillation detector and the pulses from the NaI(Tl) detectors resulting from the 141 keV gamma-ray energy emanating from the decays of the  $^{99m}\text{Tc}$  radionuclides. According to the decay scheme data of  $^{99m}\text{Tc}$  [4] the time-correlated pulses from the liquid scintillation detector with 141 keV gamma-ray energy are due to conversion electrons of about 2 keV energy produced from the gamma transitions from the 143 keV level to the level of  $^{99}\text{Tc}$ . Such a small energy deposit in the cocktail yields, on average, a single photoelectron at the photocathode windows of the PM tubes. This results in an extremely low detection efficiency of the LS detector. Therefore, for reliable activity determinations of  $^{99m}\text{Tc}$ , the efficiency extrapolation technique of varying the detection threshold of the LS detector requires that the single photo-electron peaks in the pulse-height spectra of the LS detector should be discriminated from the pedestal, and that the contribution from thermally-generated electrons to the single-electron peaks should be minimized.

The thermal and electronic noise occurring mainly in the single photo-electron peaks in the pulse-height spectra is greatly reduced by requiring additional  $\beta-\beta$  coincidence. The  $\beta-\beta$  coincidence is the timing correlation between the two sequences of pulse generated from the dynode outputs of the two PM tubes. Most noise pulses are not time-correlated between the two PM tubes. Only those LS pulses arriving within 0.5  $\mu\text{s}$  coincidence resolving time from the two LS signal streams are selected; their pulse-heights are summed, representing the deposited energies in the LS detector. The values of dead time used are 1  $\mu\text{s}$  for the non-extendable scheme.

We determine the operational high voltages for the PM tubes and the amplifier gains in such a way to obtain the maximum sensitivity for the single photo-electron detection. We test the sensitivity by looking at the resultant pulse-height spectra obtained with an LED shining on the photocathodes. Another more realistic test for the single-electron sensitivity is to use a  $^{113}\text{Sn}$  liquid scintillation source. The electron energies from  $^{113}\text{Sn}$  radioactivity are broadly grouped into three ranges: 3, 24 and 370 keV range. Figure 1 shows the pulse-height distribution of the  $^{113}\text{Sn}$  liquid scintillation source. The distribution is the sum of two dynode pulses in coincidence with each other. Three peaks corresponding to the three energy ranges of  $^{113}\text{Sn}$  can be discriminated. The 3 keV peak being the single-electron peak is clearly separable from the 24 keV peak, which demonstrates the good sensitivity of the LS detector to a small energy deposit of radiation. The resultant high voltage values for both the PM tubes are set to 2.7 kV.

The eight active sources are each counted for 10 min and the two blank sources for 20 h. Typical count rates of the LS detector are about  $2000\text{ s}^{-1}$  for the active sources and about  $6\text{ s}^{-1}$  for the blank sources. For one typical source, Fig. 2a and b present the pulse-height distributions of the two LS channels, Fig. 2c shows the distribution of the sum of coincident pulses of the two LS channels, and Fig. 2d displays the pulse-height distribution of the gamma

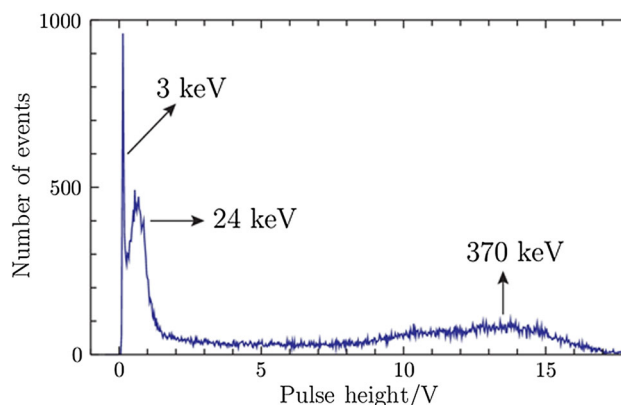
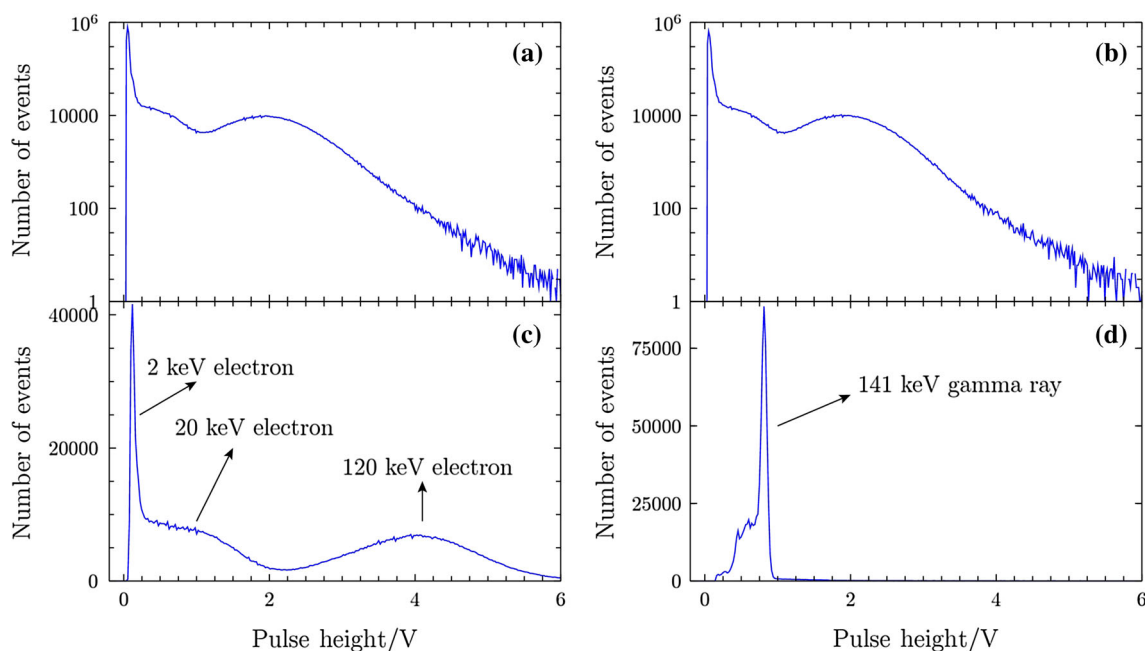


Fig. 1 Pulse-height distribution of the  $^{113}\text{Sn}$  liquid scintillation source



**Fig. 2** Pulse-height distributions for the  $^{99\text{m}}\text{Tc}$  pulses. **a** and **b** Two dynode signals of the beta channels. **c** Sum of the two coincident dynode signals of the beta channels. The 2 keV electron events are

channel. The 141 keV gamma-ray peak in Fig. 2d is evident. The single-electron peak in Fig. 2c is greatly reduced in comparison with those of Fig. 2a and b owing to the coincidence requirement of the two LS channels.

Present in Fig. 2c are the two broad peaks in addition to the single-electron peak. The two broad peaks are expected to be due to the about 20 keV Auger electrons and about 120 keV conversion electrons from  $^{99\text{m}}\text{Tc}$  decays. Since the 120 keV conversion electrons emanate from the gamma transitions from the 141 keV energy level to the ground level of  $^{99\text{m}}\text{Tc}$ , they are not in coincidence with the 141 keV gamma-rays. Figure 3 shows the pulse-height distribution of only those pulses of Fig. 2c accompanied by

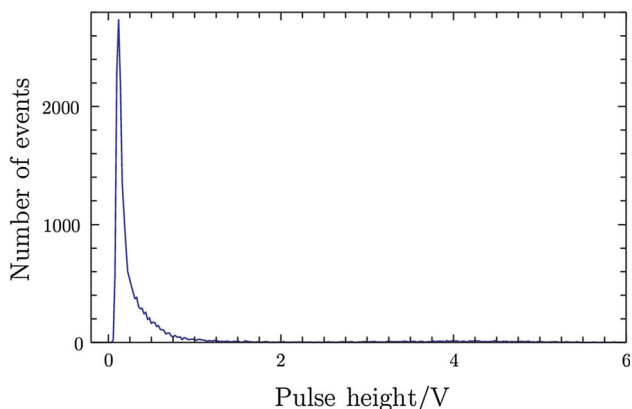


**Fig. 3** Sum of the heights of the coincident dynode signals of the two LS channels in coincidence with the 141 keV gamma pulses

populated at the single electron peak near the zero pulse height region. **d** Sum of the two gamma channels

the coincident gamma pulse from the full-absorption gamma window. Indeed only the 2 keV conversion electrons and a small number of 20 keV Auger electrons survive the coincidence requirement.

The beta spectrum of Fig. 2c, the gamma spectrum of Fig. 2d and the coincidence spectrum of Fig. 3 are used to derive the observed beta, gamma and coincidence count rates at various values of discrimination level applied for the beta spectrum. For each threshold value various rate-dependent systematic effects such as dead time, coincidence resolving time and out-of-channel effects are corrected to obtain the true beta rate  $\rho_\beta$ , the true gamma rate  $\rho_\gamma$  and the true coincidence rate  $\rho_{\beta\gamma}$ . The data points to be extrapolated for activity determination are the experimental values of  $\rho_\beta\rho_\gamma/\rho_{\beta\gamma}$  as a function of  $\rho_\gamma/\rho_{\beta\gamma}-1$  at various discrimination levels. The standard uncertainties of data points due to random effect are evaluated from the standard deviations obtained by repeating the experiments. Correlations between all data points are also taken into account during the extrapolation procedure, giving an unbiased estimate of the fitted parameters and their covariance. Figure 4 shows  $\rho_\beta\rho_\gamma/\rho_{\beta\gamma}$  as a function of  $\rho_\gamma/\rho_{\beta\gamma}-1$  for one  $^{99\text{m}}\text{Tc}$  source and a superimposed linear fit obtained using a generalized least-squares method. The range of pulse-height discrimination levels used in this fit is from 60 to 220 mV, which corresponds to 5–2% in the value of the observed beta-ray detection efficiency  $\varepsilon_\beta$  seemingly determined by  $\rho_{\beta\gamma}/\rho_\gamma$ . The measured activity is obtained from the y-axis intercept of the fitted line, which turns out

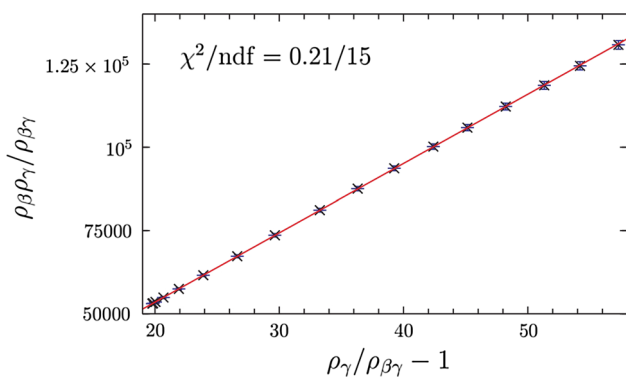


**Fig. 4** Efficiency extrapolation for  $^{99\text{m}}\text{Tc}$

to be  $(11.90 \pm 0.19)$  kBq. The quoted uncertainty is the standard uncertainty evaluated by the Chi square method [5] representing the repeatability of the result. The specific activity is derived using the mass of transferred active solution for the source.

The above mentioned procedure is applied to all of the prepared LS sources. The measured specific activity value for each source is corrected for the half-life decay of  $^{99\text{m}}\text{Tc}$  to a reference date. Table 1 summarizes the decay-corrected specific activity values along with their standard uncertainties for both the four Ultima Gold sources and the four Hionic Fluor sources. The beta-ray detection efficiencies used for the linear fits are also indicated in the table. The maximum beta-ray efficiencies used for the Ultima Gold data is 5%, whereas those of the Hionic Fluor cocktail are limited to 3% owing to the low light output of the cocktail. Consequently, the evaluated uncertainties for the Hionic Fluor sources are much larger than those for the Ultima Gold sources.

An arithmetic average of the specific activity over the four Ultima Gold sources gives a mean specific activity of  $18.532 (72)$  MBq  $\text{g}^{-1}$ . This value is about 1% different from the mean specific activity calculated from the Hionic Fluor sources.

**Table 1** Measured values of the  $^{99\text{m}}\text{Tc}$  specific activity using the DCC method along with their standard uncertainties due to the random effect

Source number	Fit range in $\varepsilon_{\beta}$ (%)	Specific activity (MBq $\text{g}^{-1}$ )
UG-1	2–5	18.44 (30)
UG-2		18.68 (51)
UG-3		18.39 (33)
UG-4		18.62 (38)
HF-1	2–3	18.7 (49)
HF-2		19.0 (37)
HF-3		18.4 (52)
HF-4		19.0 (43)

### Triple-to-double coincidence ratio counting

The same LS sources are counted using the KRISS TDCR system. We measure each source for 10 s, repeat each measurement 30 times, and obtain a TDCR parameter defined as a ratio of the sum of the triple-coincidence events to the logical sum of double-coincidence events. The extendable dead time scheme is used with base dead time of 20  $\mu\text{s}$ . The operational voltages of the three PM tubes are set to 2.8 kV with a typical double-coincidence count rate of  $160 \text{ s}^{-1}$ . The coincidence resolving times used are 10 ns. The measured TDCR parameter is, on average, 0.79 and 0.82 for the Ultima Gold sources and the Hionic Fluor sources respectively. No efficiency variations are performed for this measurement.

We calculate the double-coincidence efficiency and triple-coincidence efficiency for  $^{99\text{m}}\text{Tc}$  as a function of the TDCR parameter. The calculation is based on the Poisson distribution for the number of photoelectrons in the PM tubes. The ionization quenching is corrected by using the Birks formula with Birks kB as a free parameter. The stopping power of electrons in the LS cocktail, which is necessary for the Birks formula, is calculated from the formula for the linear energy transfer of electrons.

The radioactive decay of  $^{99\text{m}}\text{Tc}$  is simplified into the following four decay paths: internal conversion (level 2  $\rightarrow$  level 1) + internal conversion (level 1  $\rightarrow$  level 0); internal conversion (level 2  $\rightarrow$  level 1) + 141 keV gamma-ray emission (level 1  $\rightarrow$  level 0); internal conversion (level 2  $\rightarrow$  level 0); 143 keV gamma-ray emission (level 2  $\rightarrow$  level 0). We calculate the double-coincidence and triple-coincidence efficiency for each path and add them weighted with the branching ratios. The calculated TDCR parameter is the ratio of the total triple-coincidence efficiency to the total double-coincidence efficiency. The KLM shell model is used to simulate the rearrangement of atomic electrons of  $^{99}\text{Tc}$  following the internal conversion decay. The PENELOPE Monte Carlo simulation software [6] is used to simulate the interaction of the X-rays and gamma-rays of  $^{99\text{m}}\text{Tc}$  with the LS detector and obtain the energy distribution of electrons produced by the interactions. The energy distributions along with other electrons are then used to calculate the efficiency values and the TDCR parameter.

We find that the mean value of the deposition energy per one  $^{99\text{m}}\text{Tc}$  decay in the LS is only 20 keV out of 143 keV  $^{99\text{m}}\text{Tc}$  decay energy. Of this 20 keV the gamma-ray contribution amounts to only 3 keV, with the remaining 17 keV being from the conversion electrons. The fraction of gamma-ray contribution to the total available energy, considered as indicating the uncertainty level of the calculated uncertainty is 15%. This value should be compared

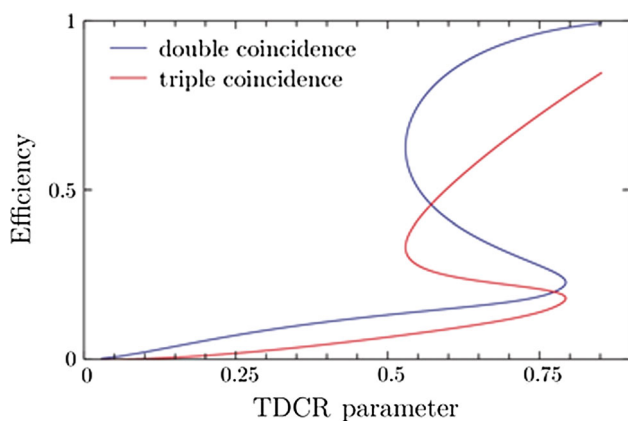


**Fig. 5** Calculated double-coincidence and triple-coincidence efficiencies of  $^{99m}\text{Tc}$  function of the calculated TDCR parameter

with the same quantities of 83 and 60% corresponding, respectively, to  $^{54}\text{Mn}$  and  $^{65}\text{Zn}$ . This difference suggests that the calculated efficiencies of  $^{99m}\text{Tc}$  are relatively accurate among the electron capture decaying radionuclides. Figure 5 shows the calculated double-coincidence and triple-coincidence efficiencies of  $^{99m}\text{Tc}$  as a function of the calculated TDCR parameter. The calculation is based on the simulation of the Ultima Gold cocktail with kB

value equal to  $0.0025 \text{ cm MeV}^{-1}$ . From the figure we see that the calculated double-efficiency value corresponding to the mean experimental TDCR parameter of 0.79 is 24%.

We obtain the experimental TDCR parameter and double-coincidence count rate for each active source of the Ultima Gold cocktail, and we determine the value of the double-coincidence efficiency corresponding to the TDCR parameter from Fig. 5. Then we calculate the activity using the double-coincidence count rate and the double-coincidence efficiency value for each source. Radioactive decays are corrected to the same date as applied in the digital coincidence counting. The mean of the measured specific activities of the four Ultima Gold sources, along with its standard deviation, is  $18.491(94) \text{ MBq g}^{-1}$ . The same procedure applied to the Hionic Fluor sources gives a mean specific activity  $18.390(80) \text{ MBq g}^{-1}$ . However, in this case the calculation is performed at a different kB value of  $0.007 \text{ cm MeV}^{-1}$ . The standard uncertainty of the calculated efficiency due to the choice of kB value is estimated to be about 3% by varying the kB value within a reasonable range. Additional 1% standard uncertainty due to the random uncertainty of the experimental TDCR value should be combined into the total standard uncertainty of the calculated efficiency.

**Table 2** Results of the specific activity measurements along with their measurement variability due to replicated measurements evaluated at a coverage factor of  $k = 1$

Method	LS cocktail	Specific activity ( $\text{MBq g}^{-1}$ )
DCC with $\beta$ - $\gamma$ coincidence system	Ultima Gold	18.532 (72)
	Hionic Fluor	18.76 (15)
TDCR	Ultima Gold	18.491 (94)
	Hionic Fluor	18.390 (80)

**Table 3** Uncertainty components evaluated in the determination of  $^{99m}\text{Tc}$  specific activity by DCC with Ultima Gold cocktail

Uncertainty contributions due to	Comment	Evaluation method	Relative standard uncertainty (%)
Reproducibility with different sources	Estimated standard deviation of the mean of the activity values of the four active sources and one blank source	A	0.384
Reproducibility with different fit ranges	Estimated standard deviation of a priori distribution obtained by using different ranges of the beta-ray detection efficiency	B	0.699
Reproducibility with different $\beta$ - $\beta$ coincidence resolving time	Estimated standard deviation of a priori distribution obtained by using different values of resolving time for $\beta$ - $\beta$ coincidence signals	B	0.297
Mass determination uncertainty	Estimated standard uncertainty of mass measurement of the amount of an active solution transferred to an LS vial	B	0.050
$^{99m}\text{Tc}$ half-life uncertainty	Standard uncertainty on decay correction over the decay interval	B	0.063
$^{99}\text{Mo}$ impurity	Estimated standard uncertainty evaluated by taking into account the minimum detectable activity of the HPGe detector measuring the $^{99m}\text{Tc}$ solution	B	0.010
Combined standard uncertainty	0.856		



## Results and discussion

Table 2 recapitulates the results of the specific activity measurements along with their measurement variability due to replicated measurements evaluated at a coverage factor of  $k = 1$ . Since the result with Ultima Gold from the DCC has a much lower uncertainty level than the other results, we adopt the result from DCC with Ultima Gold as the reference value of  $^{99m}\text{Tc}$  measurement. Table 3 lists the uncertainty components in the result for the specific activity measurement by DCC with Ultima Gold cocktail.

## Conclusion

The K4 comparison result shows that the KRISS primary standard for  $^{99m}\text{Tc}$  activity lies within the standard uncertainty with the Key Comparison Reference Value defined from other  $^{99m}\text{Tc}$  measurements [7]. Thus any KRISS-traceable measurement results for  $^{99m}\text{Tc}$  activity have metrological comparability, being traceable to the common reference of the definition of the SI unit of activity “Bq”.

## References

1. Lee KB, Lee JM, Park TS, Oh PJ, Lee SH, Lee MK (2011) Application of digital sampling techniques for  $4\pi\beta(\text{LS})-\gamma$  coincidence counting. Nucl Instrum Methods Phys Res, Sect A 626–627:72–76
2. Lee KB, Lee JM, Park TS, Lee SH (2010) Development of a high-efficiency  $4\pi\beta(\text{LS})-\gamma$  coincidence system for direct measurements of activity in radioactive decay. IEEE Trans Nucl Sci 57(5):2613–2616
3. Lee KB, Lee JM, Park TS, Hwang HY (2004) Implementation of TDCR method in KRISS. Nucl Instrum Methods Phys Res, Sect A 534(3):496–502
4. DDEP (2004) Decay data evaluation project data. [http://www.nucleide.org/DDEP\\_WG/Nuclides/Tc-99m\\_tables.pdf](http://www.nucleide.org/DDEP_WG/Nuclides/Tc-99m_tables.pdf)
5. Lee KB, Lee JM, Park TS, Lee SH (2010) Construction of classical confidence regions of model parameters in nonlinear regression analyses. Appl Radiat Isot 68(7–8):1261–1265
6. Bar J, Sempau J, Fernandez-Varea JM, Salvat F (1995) Penelope: an algorithm for Monte Carlo simulation of the penetration and energy loss of electrons and positrons in matter. Nucl Instrum Methods Phys Res, Sect B 100(1):31–46
7. Michotte C, Park TS, Lee KB, Lee JM, Lee SH (2012) Comparison of  $^{99m}\text{Tc}$  activity measurements at the KRISS using the new SIRTI of the BIPM. Appl Radiat Isot 70(9):1820–1824